

Final report

OTKA K 124862 grant: Novel mechanisms of maternal-fetal immune regulation in early pregnancy: the role of placental proteins in extracellular vesicle-mediated immune modulation”

Summary

With the support of this OTKA grant, we 1) published 21 peer-reviewed manuscripts (total IF: 104), 2) co-edited a highly cited research topic in *Frontiers in Immunology*, one of the best cited journals in the field, which received >330,000 views in total and was also published as an e-Book (Fig. 1), 3) published top downloaded/cited papers in this prestigious journal, 4) got on the cover of *Placenta* with another publication (Fig. 2), 5) discovered several physiological and pathophysiological signaling events related to placenta- and embryo-derived soluble and extracellular vesicle (EV)-bound proteins. These results are summarized below according to work-packages.

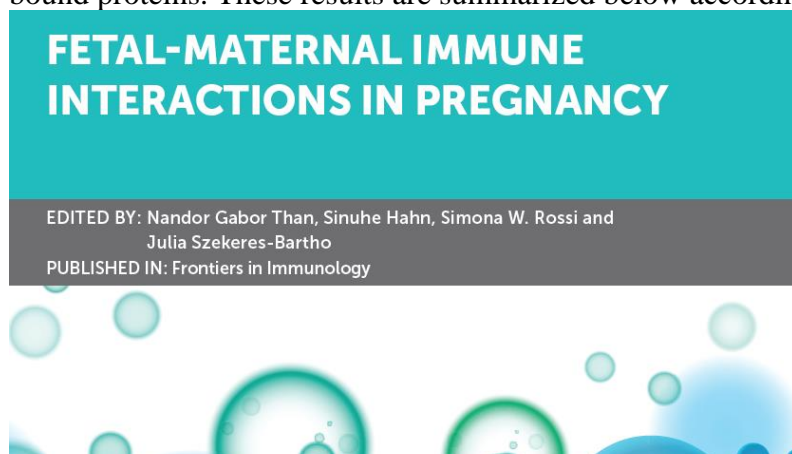


Figure 1. Cover of *Frontiers in Immunology* e-Book



Figure 2. Cover of *Placenta*

WP0 - Blood collection and tEV isolation

Blood from pregnant women with healthy pregnancies and miscarriages (n=100) was collected in 1st trimester. Plasma samples were separated and stored in ULT freezers. These are used for extracellular vesicle (EV) isolation and characterization.

WP1 - Detection of embryonic/placental protein expressing EVs in maternal blood

Maternal plasma collected in 1st trimester from women with healthy pregnancies or miscarriages was used to isolate EVs. Flow cytometric detection of circulating placental origin EVs was performed. We carried out studies on the placental expression of embryonic/placental proteins (PPs) in healthy and disease conditions (Fig. 3, Ref 1-4). The preselection of proteins (PP1, -5, -8, -13/gal13, -22, MP4, gal14) for the functional study was based on their placental expression by qRT-PCR or their presence on placental EVs by flow cytometry (Refs 1-4). Gal13/gal14 had the most promising value for further studies.

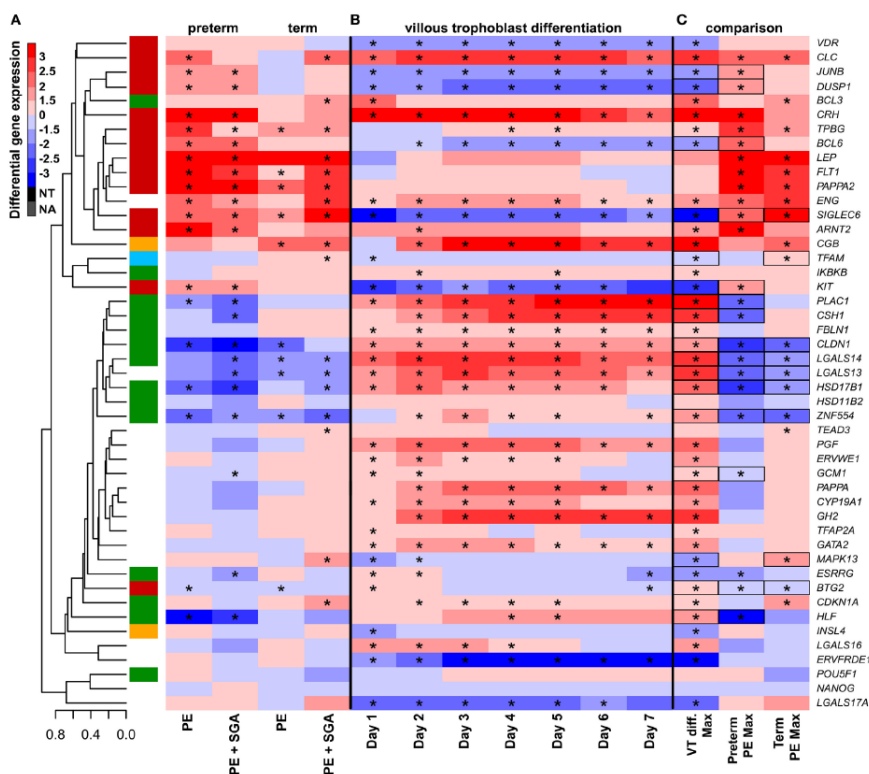


Figure 3. The effect of trophoblast differentiation on differentially expressed genes in preeclampsia.

(a) Hierarchical clustering tree of expression data for 47 genes in 100 placental specimens was augmented with a heatmap representing differential gene expression in term or preterm subgroups of preeclampsia. (B) Primary villous trophoblast (VT) differentiation time series expression data for 47 genes were depicted with a heatmap representing differential gene expression in each time point (days 1–7) compared to day 0. (c) Maximum expression values in the VT differentiation time series were presented alongside with maximum expression values in the placenta in preterm or term preeclampsia. Comparative visualization revealed the opposite-direction differential regulation of 17 genes in preeclampsia compared to VT

differentiation as depicted with black boxes. Among these genes, 15 had this behavior in preterm preeclampsia and 9 in term preeclampsia ($p = 0.057$). In (a–c), stars depict significant changes, color bar encodes signed (up or down)-fold changes. Abbreviations: NA, not expressed; NT, not examined (Ref 1).

Publications:

- 1) Than et al, *Front Immunol*, 9, 1661, 2018, IF: 4.7, SCImago: D1
- 2) Karaszi et al, *Placenta*, 76, 30, 2019, IF: 3.2, SCImago: Q1
- 3) Szenasi et al, *Peer J*, 7, e6982, 2019, IF: 2.4, SCImago: Q1
- 4) Szabo et al, *Placenta*, 99, 197, 2020, IF: 3.5, SCImago: Q1

WP2 - Identification of immune cell targets of embryonic/placental protein expressing EVs

Placenta-specific galectin-induced overexpression in BeWo cells was established/validated by qRT-PCR and flow cytometry. BeWo-derived EVs were isolated by size exclusion chromatography or differential centrifugation, methods optimized and validated by ISEV recommendation. Validation of the method was by flow cytometric detection of the exofacial molecular pattern of EVs and by the analysis of the size distribution of isolated EVs. Bead-assisted flow cytometry was evaluated for the detection of small-sized EVs.

BeWo-derived EVs bound to T cells and had stronger binding to Th cells. EV binding was blocked by anti-PSR antibody or Annexin V, denoting the role of phosphatidylserine (PS)-PS receptor interaction in BeWo-EV binding. Circulating EVs from pregnant women's plasma bound to T cells. Circulating intermediary-sized EV pattern of healthy pregnant women was analyzed by multicolor flow cytometry. Trophoblast-derived EVs were identified on their exofacial HLA-G expression. The percentage of gal14+ EVs was significantly higher in plasma from women with miscarriage than in gestational age-matched healthy controls.

WP3 - Investigation of the effects of embryonic/placental protein expressing tEVs on target adaptive and innate immune cells

The functional activities of trophoblastic EVs were investigated using BeWo cell-lymphocyte co-cultures with 1µm inserts. We proved that: 1) cytokine production of lymphocytes changes in co-culture systems; 2) BeWo-derived EVs modified IL6Rα expression of Th cells; 3) BeWo-derived EVs induced IL10 production in Th cells, 4) BeWo cells and lymphocytes had an impact on NK cell cytolytic activity.

Intermediary-sized vesicles (iEVs) derived from placenta-specific galectin overexpressing BeWo cells were characterized by their surface galectin expression. Galectin expressing iEVs induced apoptosis in circulating lymphocytes.

Earlier we proved that BeWo-derived EVs shift the polarization of Th cells into regulatory phenotype. Now we showed that EV-associated HSPE1 (using CRISPR-Cas9 based HSPE1 KO BeWo cells) induces Treg development (Ref 5). We distinguished 7 Treg subtypes and showed that the expression of HSPE1 is Treg subtype dependent using single cell transcriptomics. CAPG expression was characteristic of the T memory phenotype. In conclusion, HSPE1 and CAPG may be used as markers for the identification of Treg subtypes (Fig. 4, Ref 5).

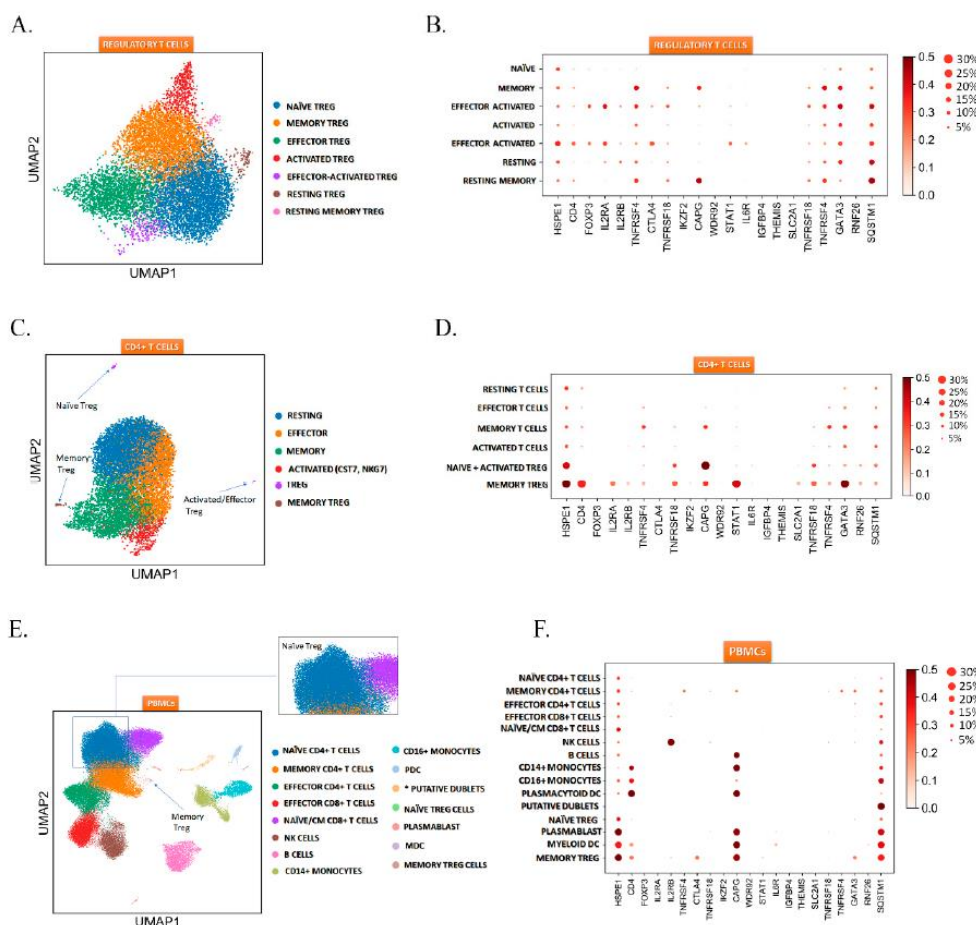


Figure 4. Regulatory T cell heterogeneity revealed by single cell transcriptomics. (A) UMAP clustering of Treg cell subsets. (B) Treg cell subtype dependent expression of HSPE1. (C) UMAP clustering of CD4+ T cell subsets, blue arrows showing identified Treg cell subsets. (D) CD4+ T cell subsets dependent expression of HSPE1. (E) UMAP clustering of PBMCs, blue arrow showing memory Treg cell population and green points showing naive Treg cell population dispersed in CD4+ naive cells. (F) PBMCs subsets dependent expression of HSPE1 (Ref 5).

Publication:

5) Kovacs et al, *Int J Mol Sci*, 20, 2019. IF: 4.2, SCImago: Q1

WP4 - Characterization of the effects of embryonic/placental proteins on adaptive and innate immune cells at the molecular level

T cells expressed SHBG, and B-, T cells bound and internalized external SHBG, a process that is decreased in B cells in pregnant compared to non-pregnant women. SHBG receptor candidates expressed by lymphocytes were identified *in silico*, including ER α . Recombinant SHBG promoted estradiol uptake by lymphocytes and influenced Erk1/2 phosphorylation. SHBG-SHBG receptor membrane ER complex participated in rapid estradiol signaling in lymphocytes, and this pathway was altered in B cells in pregnant women (Ref 6).

Gal13/gal14 was expressed by the syncytiotrophoblast (STB) in 1st trimester, and their placental expression was decreased in miscarriages (Fig. 5). Recombinant gal13/gal14 bound to T cells and induced apoptosis of Th and Tc cells. Gal13/gal14 altered cell surface expression of activation markers on T cells: CD71 is decreased by gal14, CD25 is increased by gal13, and CD95 is increased by both galectins. Non-activated T cells produced larger amounts of IL8 in presence of gal13/gal14. Overall, gal13/gal14 may provide an immune privileged environment at the maternal-fetal interface, and their reduced expression is related to miscarriages (Refs 7-8).

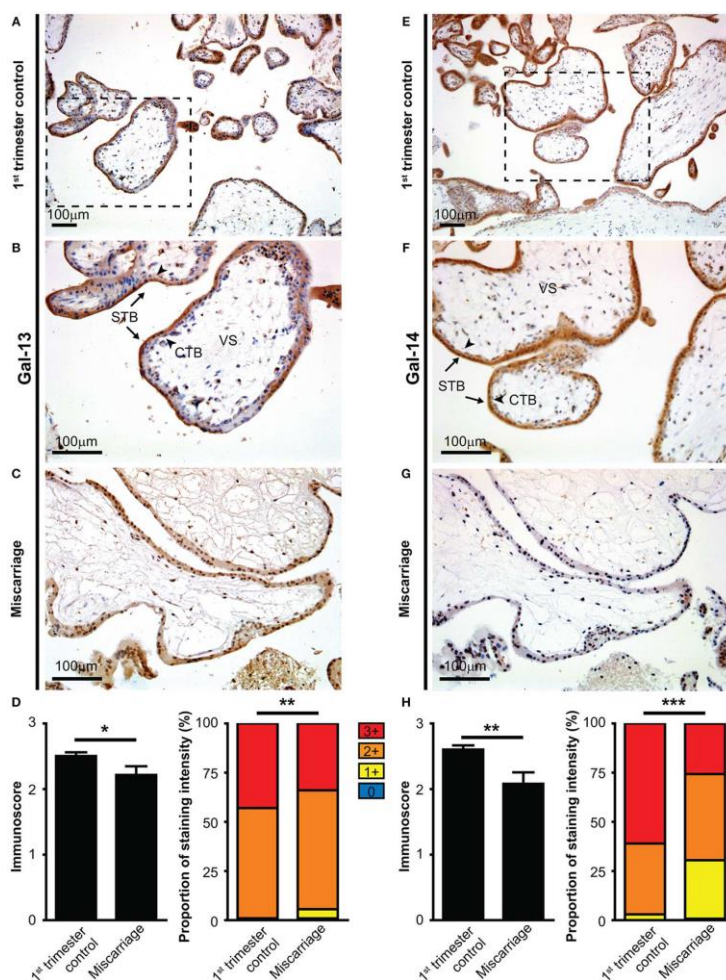


Figure 5. The syncytiotrophoblast expresses galectin-13 and galectin-14 in the first-trimester placenta, which is decreased in miscarriage. Five-micrometers-thick first-trimester placental sections from normal pregnancy (A,B,E,F) or from miscarriage (C,G) were stained for Gal-13 (A–C) or Gal-14 (E–G) by specific monoclonal antibodies. Chorionic villi exhibited intense syncytiotrophoblast cytoplasmic staining (arrows, STB), while the villus stroma (VS) and cytotrophoblasts were negative (arrowheads, CTB). Representative images, hematoxylin counterstain, 100x (A,E) and 200x (B,C,F,G) magnifications. Gal-13 (D) and Gal-14 (H) immunoscores (mean ± SEM) and proportion of staining intensities in control placentas (n = 30) and placentas with miscarriage (n = 10) are displayed on left and right graphs, respectively (Gal-13: $n_{\text{total villus}} = 775$ and $n_{\text{total villus}} = 106$, respectively; Gal-14: $n_{\text{total villus}} = 797$ and $n_{\text{total villus}} = 121$, respectively). Unpaired t-test was used for the comparison of the mean immunoscores of the two groups. Fisher's exact test was performed to test the frequency difference of Gal-13 or Gal-14 immunostaining between control and miscarriage groups (* $p < 0.05$, ** $p < 0.01$, *** $p < 0.001$) (Ref 7).

Gal13 inhibited apoptosis of neutrophils and increased PDL1, HGF, TNF α , MMP9 expression and ROS production. Gal13-treated neutrophils turned into a phenotype that supports placental and vascular expression growth and inhibits T cell functions, which are important for proper placental functions and maintenance of immune tolerance (Ref 9).

Microarray study of villous trophoblasts showed increasing gal13/gal14 expression during trophoblast differentiation. We described gene modules and clusters involved in this dynamic differentiation. Immune defense functions were first established, followed by structural and metabolic changes, and then by peptide hormone synthesis. We described key transcription factors that regulate

gene modules involved in placental functions and we also inferred how villous trophoblast differentiation and functions are dysregulated in preterm preeclampsia (Fig. 6, Ref 10).

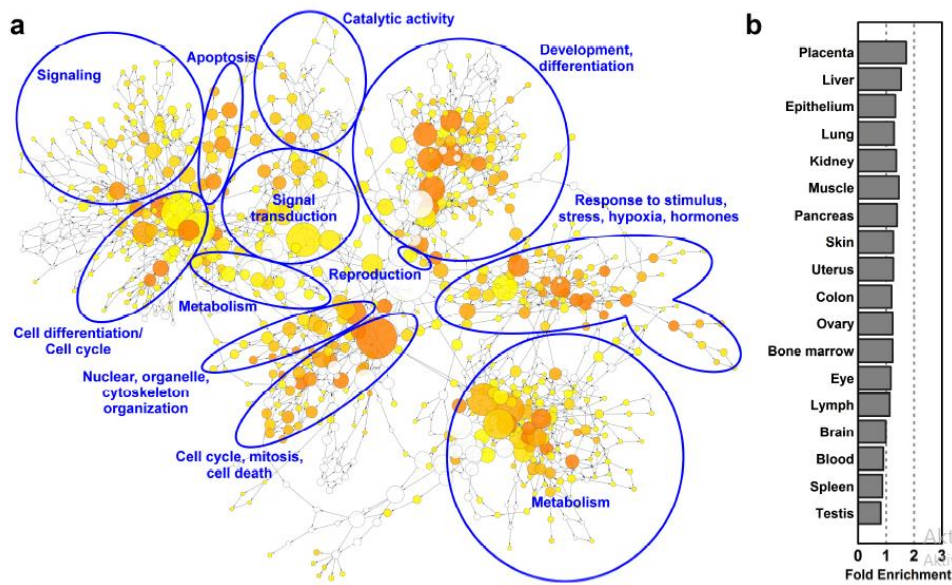


Figure 6. Gene-regulatory networks, biological processes and tissue enrichments in differentiating villous trophoblasts. (a) The network of biological processes enriched among differentially expressed (DE) genes was created by BiNGO and visualized with Cytoscape. Sizes of the circles relate to the number of genes involved in the biological processes and colors refer to p-values. The groups of most enriched biological processes were manually circled and labeled. The color code depicts p-values. (b) The UniProt tissue enrichments among DE genes were assessed with DAVID and are represented in a bar chart in the order of their enrichment significance value (Ref 10).

values. (b) The UniProt tissue enrichments among DE genes were assessed with DAVID and are represented in a bar chart in the order of their enrichment significance value (Ref 10).

We optimized recombinant gal expression using various *E. coli* strains and did not see the difference in their effect on PBMC viability and apoptosis. We optimized NK cell purification, but we could achieve better results with PBMCs using population marker antibodies. Gal-treatment increased the viability of PBMCs, decreased the proportion of apoptotic T-, B-, NK cells, and monocytes, had no effect on T-, NK cell proliferation, increased IL8, IL10, and IFN γ production, and induced Erk1/2, p38, and NF- κ B phosphorylation. These suggest that gal13/gal14 alter cell viability and cytokine production, probably with the involvement of MAPK and NF- κ B signaling pathways, important for the proper immune environment in pregnancy (Ref 11).

Using primary trophoblasts, 3D organoids, and CRISPR-Cas9 genome-edited JEG3 clones, we showed that YAP promotes maintenance of villous cytotrophoblasts. Genetic or chemical manipulation of YAP stimulated proliferation and expression of cell cycle regulators and stemness-associated genes, but inhibited cell fusion and production of STB-specific proteins (e.g. galectins) suggesting that YAP has a pivotal role in the maintenance of the human placental trophoblast epithelium (Ref 12).

By RNA-Seq, we demonstrated decreased expression of gal13/gal14 in complete moles compared to healthy 1st-trimester placentas. We found 3,729 differentially expressed genes in total and the enrichment of placenta-specific genes as well as genes involved in imprinting and immune processes. Nearly half of the 38 altered KEGG pathways were associated with immune processes, suggesting a complex change in placental development and immune processes in complete moles (Ref 13).

As a continuation of this work, the analysis of genome-wide DNA methylation and transcriptome data revealed that DNA methylation increases with disease severity in gestational trophoblastic diseases, principally influencing the gene expression of villous trophoblast differentiation-related or predominantly placenta-expressed genes. In complete moles, we found slight upregulation of DNMT3B protein, a developmentally important de novo DNA methylase, which is strongly overexpressed in choriocarcinoma cells that may partly be responsible for the large DNA methylation differences. Differentially expressed genes are mainly upregulated in moles while predominantly downregulated in choriocarcinoma (Refs 14).

A brief overview was provided on how the classification and early diagnosis of preeclampsia have progressed, focusing on studies utilizing transcriptomics and proteomics methods and including our own systems biology studies. Molecular subclasses of preeclampsia were discovered by our group based on proteomics studies, and their biomarkers and disease pathways were identified. These findings may promote the development of novel diagnostic tools for the distinct subtypes of preeclampsia syndrome, enabling early detection, personalized follow-up, and tailored care of patients (Refs 15-17).

An overview of the expression of proteoglycans' - potential galectin interaction partners - and their functional role in the placenta, in trophoblast development, and in pregnancy complications, was summarized, focusing on one of the most important members of this family, syndecan-1 (SDC1). Microarray analysis showed that among 34 placentally expressed proteoglycans, SDC1 production is markedly the highest in the placenta and that SDC1 is the most upregulated gene during villous trophoblast differentiation. Placental transcriptomic data identified dysregulated proteoglycan genes in preeclampsia and in fetal growth restriction, including SDC1, which is supported by the lower concentration of syndecan-1 in maternal blood in these syndromes. Syndecan-1 may serve as a useful marker of syncytialization and a prognostic marker of adverse pregnancy outcomes (Fig. 7, Ref 18).

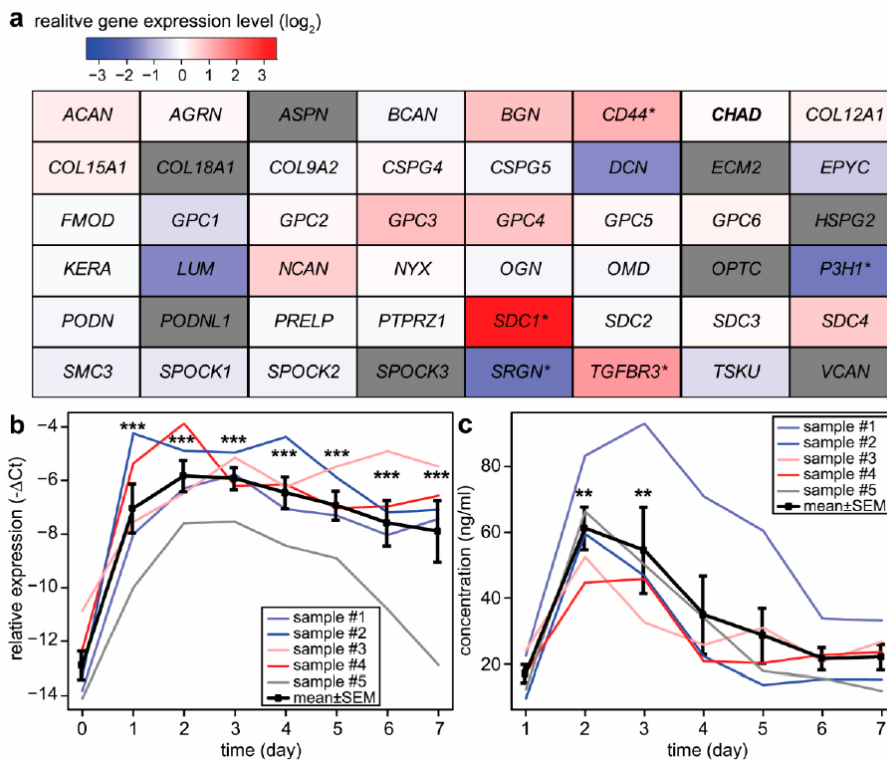


Figure 7. Changes in proteoglycan gene expression during villous trophoblast differentiation. (a) Microarray data were obtained from primary villous trophoblast cells isolated from third-trimester normal placentas ($n = 3$) during a seven-day differentiation period. The largest differences in gene expression compared to day 0 were visualized on a heatmap. Color code depicts \log_2 gene expression ratios. Grey color: no data were available. The original study was published by Szilagy et al. (b) SDC1 expression was monitored during villous trophoblast differentiation. qRT-PCR data were obtained from an extended set of primary villous trophoblast cells isolated from third-trimester normal

placentas ($n = 5$) during a seven-day differentiation period. Relative expression of SDC1, normalized to RPLP0, was visualized on the diagraph. (c) Changes in syndecan-1 protein concentration in cell culture supernatants ($n = 5$) were examined throughout spontaneous syncytial differentiation of primary villous trophoblast cells. One-Way ANOVA with Dunnett's post-hoc test was used for the analysis of qRT-PCR and ELISA results (* $p < 0.05$, ** $p < 0.01$, *** $p < 0.001$). Ribosomal Protein Lateral Stalk Subunit P0—RPLP0; syndecan-1—SDC1 (Ref 18).

Publications:

- 6) Balogh et al, *Sci Rep*, 9, 4, 2019, IF: 4.0, SCImago: D1
- 7) Balogh et al, *Front Immunol*, 10, 1240, 2019, IF: 5.1, SCImago: D1
- 8) Menkhorst E. et al, *Front Immunol*, 12, 784473, 2021, IF: 8.8, SCImago: D1
- 9) Vokalova et al, *Front Immunol*, 11, 145, 2020, IF: 7.6, SCImago: D1
- 10) Szilagy et al, *Int J Mol Sci*, 21, 628, 2020, IF: 5.9, SCImago: Q1
- 11) Oravec et al, *Front Immunol*, in press, 2022, IF: 8.8, SCImago: Q1
- 12) Meinhardt et al, *Proc Natl Acad Sci USA*, 117, 13562, 2020, IF: 11.2, SCImago: D1
- 13) King et al, *Int J Mol Sci*, 20, 4999, 2020, IF: 4.6, SCImago: Q1

- 14) Szabolcsi et al, *Biomedicines*, 9, 1935, 2021, IF: 4.8, SCImago: Q1
 15) Than et al, *Placenta*, 125,10, 2022, IF:3.3, SCImago: Q1
 16) Than et al, *Nőgyógy Szül Továbbk Szeml*, XXIV(1), 6-16, 2022
 17) Than et al, *J Perinat Med*, published online, IF: 2.7, SCImago: Q2
 18) Oravec et al, *Int J Mol Sci*, 23, 5798, 2022, IF: 6.2, SCImago: Q1

WP5 - Investigation of the molecular mechanisms of eEV-associated PIBF effects on immune cells

Embryo-derived EVs (eEVs) in mouse embryo culture media were identified by Annexin V binding capacity, using flow cytometry. PIBF content of eEVs was determined by flow cytometry and was validated by immuno-electron microscopy (Fig. 8, Ref 19).

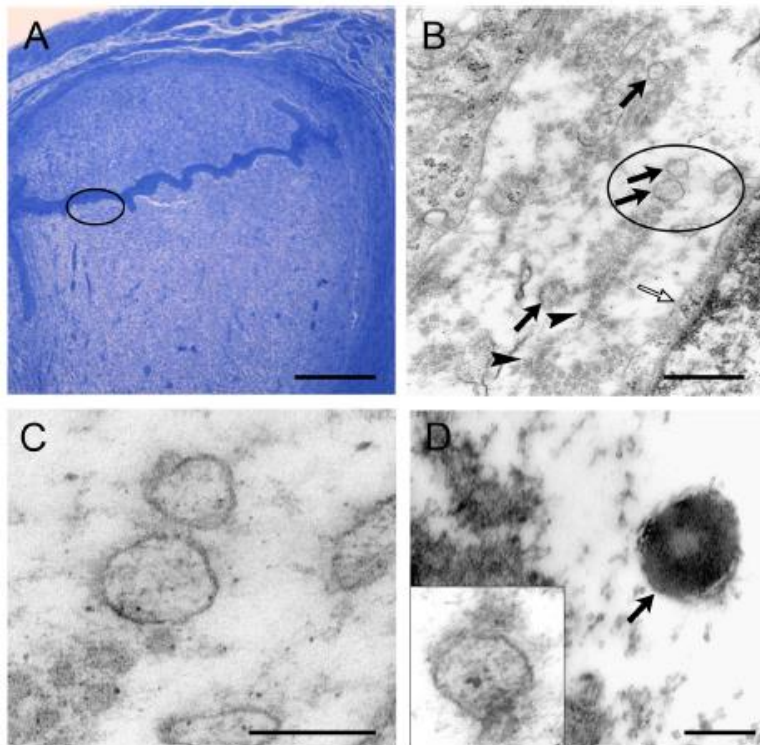


Figure 8. EVs at the feto-maternal interface and around in vitro cultured embryos. (A) Light microscopic photomicrograph showing implantation in a semi-thin section. Encircled area in A is shown with higher magnification in B. Scale bar = 200 µm. (B) Low magnification electron microscopic photomicrograph revealing EVs (arrows) at the embryo maternal interface. Open arrow point to the membrane of a maternal cell, while arrowheads indicate collagen fibres in the extracellular space. Encircled area in B is shown with higher magnification in C. Scale bar = 500 nm (C) High magnification of EVs at the embryo maternal interface. Scale bar = 200 nm. (D) In vitro cultured morula stage mouse embryos were immune-stained with rabbit anti- PIBF primary antibody, then embedded in agar and prepared for electron microscopy. The EV (indicated with an arrow) produced by the embryo is PIBF-immuno-reactive. Insert shows EV reacted with the secondary antibody only, as a negative control. Scale bar = 100 nm (Ref 19).

Mouse embryo-derived EVs adhered to the surface of Th and Tc cells, but not to non-lymphoid cells. Tc spleen cells bound more embryo-derived EVs than Th cells. Murine embryo-derived EVs increased the number of IL10+ cells among peripheral Tc cells, but not in the Th cells. Pre-treatment of EVs with anti-PIBF antibody abrogated this effect (Fig. 9, Ref 20).

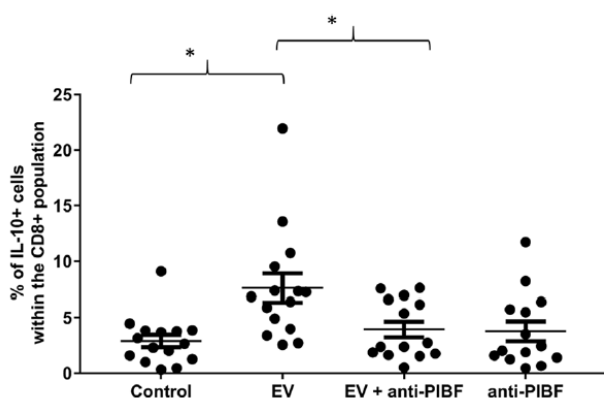


Figure 9. IL-10 expression of mouse peripheral CD8+ lymphocytes incubated with mouse embryo-derived EVs, or with anti-PIBF treated mouse embryo-derived EVs. Anti-CD8 labelled mouse spleen cells were incubated with embryo derived EVs, or with EVs that had been pre-treated with anti-PIBF antibody for 30 mins. Anti-rabbit IgG was used as an isotype control. Then the cells were labelled with anti-IL-10 antibody, and the number of IL-10 positive cells among the subpopulations was determined by flow cytometry. The bars represent the mean \pm SEM of 15 measurements. *p < 0.001 (Ref 20).

The miRNA content of mouse embryos and embryo-derived mEVs was determined by Next-Gen Seq. Target prediction was performed to identify miRNA target genes. We compared the effect of treatments with different wavelengths of light. Bioinformatics analysis of miRNA patterns and validation of results by molecular biological methods is ongoing.

Immune-checkpoint molecules and PIBF expression were measured on EVs produced by control (competent embryo model) and light-exposed (model for embryos with poor implantation capacity) cultured mouse embryos. Both immune checkpoint molecules and PIBF were expressed at a lower rate in light-stressed embryos. Murine spleen cells are incubated with EVs produced by competent- or non-implanting embryos, and NK activity and cytokine production are detected to confirm the biological importance of this finding. Initial data show, that while EVs produced by competent embryos decrease NK activity and induce IL10 production, EVs from embryos with poor implantation capacity do not (Ref 21).

The mRNA expression of Tim3 (gene: *PDCDI*) and PD1 (gene: *HAVCR2*) on Th cells and Tc cells in peripheral blood, as well as TGF β and IP10 concentrations in sera of women with recurrent miscarriage (RM), compared to gestational age-matched healthy pregnant women were characterized. *PDCDI* expression was upregulated, while *HAVCR2* expression tended to decrease in PBMCs of RPL patients, compared to controls. In line with this, the percentage of PD1-expressing Th cells and Tc cells was significantly higher, while the percentage of Tc cells expressing Tim3 was significantly lower in RM patient than in healthy controls. TGF β concentration in the sera of RM patients was lower than in those of controls and the concentration of the IP10 was higher in RM patients than in the controls (manuscript in preparation).

Publications:

- 19) Pallinger et al, *Sci Rep*, 8, 4662, 2018, IF: 4.1, SCImago: D1
- 20) Bognar et al, *J Reprod Immunol*, 132, 21, 2019, IF: 4.0, SCImago: Q1
- 21) Csabai et al, *Front Immunol*, 11, 349, 2020, IF: 7.6, SCImago: D1

Conclusions

Our findings may contribute to the better understanding of 1) the effects/roles of the investigated placental proteins in the establishment and maintenance of maternal-fetal immune tolerance in healthy pregnancies and 2) how the imbalance of these proteins may contribute to the pathophysiological events in the development of severe pregnancy complications. These results may also lead to the implication of new biomarkers of pregnancy complications (e.g. placental proteins expressed on tEVs in the maternal circulation), which may improve the accuracy of the current screening methods for pathological pregnancies.